A Bioinspired Molybdenum Catalyst for Aqueous Perchlorate Reduction

Changxu Ren[1], Peng Yang[2], Jiaonan Sun[3], Eric Y. Bi[1,4], Jacob Palmer[1], Mengqiang Zhu[2], Yiying Wu[3], and Jinyong Liu[1]*

[1]Department of Chemical and Environmental Engineering, University of California, Riverside, CA 92521, United States.

[2]Department of Ecosystem Science and Management, University of Wyoming, Laramie, WY 82071, United States.

[3]Department of Chemistry, The Ohio State University, Columbus, OH 43210, United States.

[4]Martin Luther King High School, Riverside, CA 92508, United States.

*Correspondence to: jinyongl@ucr.edu; Jinyong.liu101@gmail.com.

Abstract

The detection of perchlorate (ClO_4^-) on and beyond Earth requires ClO_4^- reduction technologies to support water purification and space exploration. However, the reduction of ClO_4^- usually entails either harsh conditions or multi-component enzymatic processes. We developed a heterogeneous Mo−Pd/C catalyst from sodium molybdate to reduce aqueous ClO_4^- into Cl^- with 1 atm H_2 at room temperature. Upon hydrogenation by H_2/Pd, the reduced Mo oxide species and a bidentate nitrogen ligand (1:1 molar ratio) are transformed *in situ* into oligomeric Mo sites on the carbon support. The turnover number and frequency for oxygen atom transfer from ClO_x^- substrates reached 3850 and 165 h^{-1} on each Mo site. This simple bioinspired design yielded a robust water-compatible catalyst for the removal and utilization of ClO_4^-.

Perchlorate (ClO_4^-) is a pervasive water contaminant on Earth (*1, 2*) and a major salt component in the surface soil on Mars (*3, 4*). Because the uptake of ClO_4^- through water and food can cause thyroid gland malfunction, ClO_4^- levels in the drinking water are regulated. NASA has also identified Martian ClO_4^- as both a potential hazard to humans and an oxygen source to supply exploration activities (*5*). However, ClO_4^- is highly inert, so that it is widely used for ionic strength adjustment in various chemical systems. The oxidizing power of ClO_4^- has been primarily utilized via rocket fuels or munitions (*1*). Here, we report on a simple yet highly active heterogeneous Mo−Pd catalyst that can reduce aqueous ClO_4^- into Cl^- with 1 atm H_2 at room temperature.

Microbes can use ClO_4^- for respiration (Fig. 1A) (*6, 7*). In the multifactor metalloenzyme system (Fig. 1B), a Mo co-factor biosynthesized from molybdate (*8*) and amino acid residues mediate the oxygen atom transfer (OAT) (*9*) from ClO_4^- (*10*). The $Mo^{IV/VI}$ redox cycling (Fig. 1C) is sustained by the electron transfer from H_2 or acetate via multiple Fe-S clusters, *heme* complexes, and electron shuttle compounds (*11*). Such complexity in biological systems challenges the design of an artificial ClO_4^- reduction system, especially in aqueous phase under ambient conditions. For example, ClO_4^- reduction by a Fe complex relied on hydrogen bonds in the secondary coordination sphere (Fig. 1D) and thus required the use of an anhydrous medium (*12, 13*). Furthermore, a single-function metal complex or isolated reductase needs special electron donors (e.g., methyl viologen, hydrazine, ferrocene, and phosphine) to sustain the redox cycle of the OAT metal (*12, 14, 15*). Therefore, a robust catalyst that can reduce aqueous ClO_4^- with H_2 is highly desirable (*16, 17*).

In our bioinspired design (Fig. 1F), Pd/C is used as the catalyst platform. The porous carbon mimics the protein pocket of the enzyme that accommodates the OAT metal site. The Pd^0 nanoparticles simplify the enzymatic electron transfer chain by directly harvesting electrons from H_2. Then the key task was to construct a highly active Mo site from molybdate ($Mo^{VI}O_4^{2-}$), the

same Mo source for the biosynthesized Mo co-factors (*8*). Polyoxometalates of aqueous molybdate (*18*) were readily adsorbed onto Pd/C within 30 min (fig. S1). The resulting heterogeneous MoO_x−Pd/C showed rapid reduction of ClO_3^- (*19*) but had negligible activity with ClO_4^-. Hence, we sought to substantially enhance the OAT activity of surface Mo sites by incorporating an organic ligand. Because biomimetic thio-coordinated Mo complexes are typically water- and oxygen-sensitive, we attempted to prepare active Mo sites *in situ* by simultaneously adding molybdate and neutral nitrogen ligands (*L*) in the water suspension of Pd/C under 1 atm H_2. This simple strategy achieved highly active ClO_4^- reduction by a series of (*L*)MoO_x−Pd/C catalysts (Table 1, figs. S2 and S3).

In general, aromatic bidentate ligands led to significantly higher ClO_4^- reduction activities than amines and monodentate pyridines. Bipyridine (*bpy*) was superior to phenanthroline and other aromatic ligands containing an imidazoline or oxazoline half moiety (Table 1, entries 17−19). Ligands with steric hindrance on the *ortho* positions (Table 1, entries 8, 9, and 20) and with a strain on the *bpy* backbone (Table 1, entry 22 versus 21) resulted in low activities. Electron-donating groups on the *para* positions (*20*) further enhanced the activity. At ambient temperature and pressure, ClO_4^- reduction by the [$(NH_2)_2bpy$]MoO_x−Pd/C catalyst (Table 1, entry 6) outperformed all abiotic catalysts reported to date (table S1). The chlorine balance was closed by ClO_4^- and Cl^-, indicating a negligible buildup of ClO_x^- intermediates (Fig. 2A). The optimal molar ratio between $(NH_2)_2bpy$ and Mo was 1:1 (Fig. 2B), and the optimal Mo content in the catalyst was 5 wt% (Fig. 2C). The reuse of the catalyst for ten times did not cause a noticeable loss of activity (Fig. 2D, fig. S4). During the ClO_4^- reduction, the ratios of leached Mo and $(NH_2)_2bpy$ into water were <1.5% and <0.2% of the total amount in the catalyst, respectively (Fig. 2E). The apparent 1st-order kinetics with 0.01−1 mM ClO_4^- and 0th-order kinetics at 1−100 mM ClO_4^- (figs. S5 and S6) support the

Langmuir–Hinshelwood model for heterogeneous catalysis (See Supplementary Text for kinetic modeling and mass transfer analysis). Notably, a 0.2 g/L loading of the catalyst reduced 99.99% of 100 mM ClO_4^- (~10 g/L) within 48 h (fig. S5c). Due to the high oxidative stress caused by ClO_x^- intermediates (*10, 21*), complete reduction of 100 mM ClO_4^- in water has not been reported by either microbial or abiotic systems. Assuming the Mo sites catalyzed the OAT with both ClO_4^- and ClO_x^- intermediates, the turnover number (TON) for the single batch and the initial turnover frequency (TOF_0) reached 3850 and 165 h^{-1}, respectively, for each Mo atom.

While enzymes use amino acid residues to facilitate the reduction of metal-bound oxyanions (*10, 22*), the carbon-supported catalyst needs external protons to enable the reaction (*19, 20*). The optimal activity was afforded by 1 mM H^+ (pH 3.0 by H_2SO_4). The reduced performance at a lower pH (Fig. 2F) was probably caused by the protonation of amino groups on $(NH_2)_2bpy$. In the presence of 0.1 M Cl^-, 2.0 M Cl^-, and 1.0 M SO_4^{2-}, the catalyst retained 57%, 5%, and 36% of activity, respectively (fig. S7 and table S2), showing promise for the reduction of ClO_4^- in brine solutions produced from ion-exchange or from reverse osmosis for water treatment (*1*). Furthermore, exposing the catalyst suspension to air did not cause irreversible deactivation. The same ClO_4^- reduction activity was recovered after resuming H_2 supply (fig. S8a), suggesting that the *in situ* prepared catalyst can be handled in air. In comparison, the Re−Pd/C catalyst using the pre-synthesized Re^V precursor (Fig. 1E) (*23*) was highly sensitive to air and would irreversibly deactivate (fig. S8b) (*24, 25*).

X-ray photoelectron spectroscopy (XPS) characterization identified the reduction of Mo^{VI} precursor into multiple oxidation states (+VI, +V, +IV, +III and +II) (Fig. 3A versus 3B). Air exposure reoxidized the low-valent species to Mo^V and Mo^{VI} (Fig. 3C). For the reduced bulk catalyst sample, Mo K-edge X-ray absorption near-edge structure (XANES) spectroscopic

analysis found the average valence of Mo to be 4.3 from the edge energy of 20011.7 eV (Fig. 3D and fig. S9) (*26*). Fitting of the extended X-ray absorption fine structure (EXAFS) spectra found two major atomic shells for Mo−O (1.99 ± 0.03 Å) and Mo−Mo (2.57 ± 0.02 Å) (Fig. 3E, table S3, and fig. S10). This short Mo−Mo distance, in comparison to the value of 3.4 Å in Mo^{VI} oxide clusters (*26*), indicates the reduction of polymeric molybdate to Mo^{IV} by Pd-activated H_2 (*19*). The Mo−Mo coordination number (CN, 0.9 ± 0.5) suggests the heterogeneity of the surface Mo species as a mixture of monomers (CN = 0), dimers (CN = 1), and polymers (CN > 1).

Notably, the use of $(NH_2)_2bpy$ ligand changed the structure and activity of MoO_x in the catalyst. Without the ligand, the MoO_x−Pd/C catalyst could not reduce ClO_4^-, and the highest ClO_3^- reduction was achieved with only 0.5 wt% of Mo (fig. S11). Thus, the additional 4.5 wt% of Mo in a 5 wt% MoO_x−Pd/C catalyst acted as the structural building block of polymeric MoO_x clusters rather than catalytic sites. The CN for Mo−Mo in MoO_x−Pd/C (1.7 ± 0.6, table S3) also indicated the dominance of polymeric MoO_x clusters (*19*). In stark comparison, the ClO_4^- reduction activity of $[(NH_2)_2bpy]MoO_x$−Pd/C showed a linear increase until reaching 5 wt% of Mo. Thus, most Mo atoms acted as catalytic sites, and the most probable structure is an oligomer with one $(NH_2)_2bpy$ coordinating with each Mo (Fig. 2B). The elevated sensitivity with concentrated Cl^- upon the use of $(NH_2)_2bpy$ (table S2) also corroborates the altered structure of MoO_x by the organic ligand. A representative dimer structure (Fig. 3F) is proposed based on the reported crystal structure of $Mo^{VI}_2O_6[(tBu)_2bpy]_2$, a byproduct from the hydrothermal reaction using MoO_3 and 4,4'-$(tBu)_2bpy$ (*27*). Such a structure allows for multi-valent transformation of Mo between +VI and +II (Fig. 3B).

Scanning transmission electron microscopy (STEM) and energy dispersive X-ray spectrometry (EDS) element mapping images indicate the ubiquitous distribution of Mo and N on

either carbon support or Pd^0 nanoparticles (Figs. 3G−3J and figs. S12−S14). The poor EXAFS fittings including Mo−Pd bonding (table S4) suggest isolated aggregation and distinct roles of Mo sites (OAT for ClO_x^- reduction) and Pd nanoparticles (electron transfer from H_2). However, the hydrogenation reaction is necessary to transform the polymeric Mo^{VI} precursors (*19*) and the free ligand into specific $[(NH_2)_2bpy]MoO_x$ structures to be reactive with ClO_4^-. For example, our cyclic voltammetry studies on the $[(NH_2)_2bpy]MoO_x/C$ material (without Pd^0 nanoparticles) between 0.37 and −1.1 V (versus the reversible hydrogen electrode) did not observe ClO_4^- reduction (fig. S15) but instead showed the reduction peaks of MoO_x and $(NH_2)_2bpy$ ligand (fig. S16). The potential allows the reduction of Mo^{VI} into Mo^V, Mo^{IV}, and Mo^{III} (*28, 29*), but the $[(NH_2)_2bpy]MoO_x$ clusters formed from the electrochemical reduction (*26*) were probably in different structures and thus not reactive with ClO_4^-.

The rapid and robust ClO_4^- reduction by a series of $(L)MoO_x$−Pd/C catalysts can be attributed to three major mechanisms similar to the microbial reduction process. First, the OAT energy barrier is lowered by the organic ligand (substituted *bpy* versus pterin in the Mo co-factor). Second, the redox cycling of Mo is sustained by the electron transfer from H_2 (enabled by the Pd^0 nanoparticle versus multiple biological metal factors). Third, the Mo-bound ClO_4^- requires the activation via protonation (externally added acid versus amino acid residues in the enzyme pocket). Mechanistic insights of this study highlight a strategy for designing bioinspired systems with common chemicals and simple approaches. Water-compatible heterogeneous catalyst systems will advance environmental and energy technologies for the removal and utilization of ClO_4^-.

Supplementary Materials:

Materials and Methods
Supplementary Text
Figures S1-S16
Tables S1-S4
References (*30-45*)

References:

1. B. Gu, J. D. Coates, Eds., *Perchlorate: Environmental Occurrence, Interactions and Treatment* (Springer Science & Business Media, 2006).

2. P. Brandhuber, S. Clark, K. Morley, A review of perchlorate occurrence in public drinking water systems. *J. Am. Water Works Assoc.* **101**, 63-73 (2009).

3. M. H. Hecht, S. P. Kounaves, R. C. Quinn, S. J. West, S. M. M. Young, D. W. Ming, D. C. Catling, B. C. Clark, W. V. Boynton, J. Hoffman, L. P. DeFlores, K. Gospodinova, J. Kapit, P. H. Smith, Detection of perchlorate and the soluble chemistry of martian soil at the Phoenix lander site. *Science* **325**, 64-67 (2009).

4. W. A. Jackson, A. F. Davila, D. W.G. Sears, J. D. Coates, C. P. McKay, M. Brundrett, N. Estrada, J.K. Böhlke, Widespread occurrence of (per)chlorate in the Solar System. *Earth Planet. Sci. Lett.* **430**, 470-476 (2015).

5. A. F. Davila, D. Willson, J. D. Coates, C. P. McKay, Perchlorate on Mars: a chemical hazard and a resource for humans. *Int. J. Astrobiol.* **12**, 321-325 (2013).

6. J. D. Coates, L. A. Achenbach, Microbial perchlorate reduction: rocket-fuelled metabolism. *Nat. Rev. Microbiol.* **2**, 569-580 (2004).

7. M. D. Youngblut, O. Wang, T. P. Barnum, J. D. Coates, (Per)chlorate in biology on earth and beyond. *Annu. Rev. Microbiol.* **70**, 435-457 (2016).

8. G. Schwarz, R. R. Mendel, M. W. Ribbe, Molybdenum cofactors, enzymes and pathways. *Nature* **460**, 839-847 (2009).

9. R. H. Holm, Metal-centered oxygen atom transfer reactions. *Chem. Rev.* **87**, 1401-1449 (1987).

10. M. D. Youngblut, C. L. Tsai, I. C. Clark, H. K. Carlson, A. P. Maglaqui, P. S. Gau-Pan, S. A. Redford, A. Wong, J. A. Tainer, J. D. Coates, Perchlorate reductase is distinguished by active site aromatic gate residues. *J. Biol. Chem.* **291**, 9190-9202 (2016).

11. M. G. Bertero, R. A. Rothery, M. Palak, C. Hou, D. Lim, F. Blasco, J. H. Weiner, N. C. J. Strynadka, Insights into the respiratory electron transfer pathway from the structure of nitrate reductase A. *Nat. Struct. Mol. Biol.* **10**, 681-687 (2003).

12. C. L. Ford, Y. J. Park, E. M. Matson, Z. Gordon, A. R. Fout, A bioinspired iron catalyst for nitrate and perchlorate reduction. *Science* **354**, 741-743 (2016).

13. M. J. Drummond, T. J. Miller, C. L. Ford, A. R. Fout, Catalytic perchlorate reduction using iron: mechanistic insights and improved catalyst turnover. *ACS Catal.* **10**, 3175-3182 (2020).

14. J. M. Hutchison, S. K. Poust, M. Kumar, D. M. Cropek, I. E. MacAllister, C. M. Arnett, J. L. Zilles, Perchlorate reduction using free and encapsulated Azospira oryzae enzymes. *Environ. Sci. Technol.* **47**, 9934-9941 (2013).

15. L. T. Elrod, E. Kim, Lewis acid assisted nitrate reduction with biomimetic molybdenum oxotransferase complex. *Inorg. Chem.* **57**, 2594-2602 (2018).

16. Y. B. Yin, S. Guo, K. N. Heck, C. A. Clark, C. L. Coonrod, M. S. Wong, Treating water by degrading oxyanions using metallic nanostructures. *ACS Sustain. Chem. Eng.* **6**, 11160-11175 (2018).

17. B. P. Chaplin, M. Reinhard, W. F. Schneider, C. Schüth, J. R. Shapley, T. J. Strathmann, C. J. Werth, Critical review of Pd-based catalytic treatment of priority contaminants in water. *Environ. Sci. Technol.* **46**, 3655-3670 (2012).

18. O. F. Oyerinde, C. L. Weeks, A. D. Anbar, T. G. Spiro, Solution structure of molybdic acid from Raman spectroscopy and DFT analysis. *Inorg. Chim. Acta* ***361***, 1000-1007 (2008).

19. C. Ren, P. Yang, J. Gao, X. Huo, X. Min, E. Y. Bi, Y. Liu, Y. Wang, M. Zhu, J. Liu, Catalytic reduction of aqueous chlorate with MoO_x immobilized on Pd/C. *ACS Catal.* ***10***, 8201-8211 (2020).

20. K. D. Hurley, Y. Zhang, J. R. Shapley, Ligand-enhanced reduction of perchlorate in water with heterogeneous Re−Pd/C catalysts. *J. Am. Chem. Soc.* ***131***, 14172-14173 (2009).

21. J. Liu, X. Chen, Y. Wang, T. J. Strathmann, C. J. Werth, Mechanism and mitigation of the decomposition of an oxorhenium complex-based heterogeneous catalyst for perchlorate reduction in water. *Environ. Sci. Technol.* ***49***, 12932-12940 (2015).

22. E. N. Mirts, I. D. Petrik, P. Hosseinzadeh, M. J. Nilges, Y. Lu, A designed heme-[4Fe-4S] metalloenzyme catalyzes sulfite reduction like the native enzyme. *Science* ***361***, 1098-1101 (2018).

23. M. M. Abu-Omar, L. D. McPherson, J. Arias, V. M. Béreau, Clean and efficient catalytic reduction of perchlorate. *Angew. Chem.* ***112***, 4480-4483 (2000).

24. Y. Zhang, K. D. Hurley, J. R. Shapley, Heterogeneous catalytic reduction of perchlorate in water with Re−Pd/C catalysts derived from an oxorhenium(V) molecular precursor. *Inorg. Chem.* ***50***, 1534-1543 (2011).

25. J. Liu, J. K. Choe, Y. Wang, J. R. Shapley, C. J. Werth, T. J. Strathmann, Bioinspired complex-nanoparticle hybrid catalyst system for aqueous perchlorate reduction: rhenium speciation and its influence on catalyst activity. *ACS Catal.* ***5***, 511-522 (2015).

26. H. Wang, S. Hamanaka, Y. Nishimoto, S. Irle, T. Yokoyama, H. Yoshikawa, K. Awaga, In operando X-ray absorption fine structure studies of polyoxometalate molecular cluster batteries: polyoxometalates as electron sponges. *J. Am. Chem. Soc.* ***134***, 4918-4924 (2012).

27. T. R. Amarante, P. Neves, F. A. A. Paz, M. Pillinger, A. A. Valente, I. S. Gonçalves, A dinuclear oxomolybdenum(VI) complex, [Mo_2O_6(4,4′-di-tert-butyl-2,2′-bipyridine)$_2$], displaying the $\{MoO_2(\mu\text{-}O)_2MoO_2\}^0$ core, and its use as a catalyst in olefin epoxidation. *Inorg. Chem. Commun.* ***20***, 147-152 (2012).

28. N. Anbananthan, K. N. Rao, V. Venkatesan, Cyclic voltammetric investigations of the reduction of Mo(VI) to Mo(IV) in 1 M sulphuric acid. *J. Electroanal. Chem.* ***374***, 207-214 (1994).

29. J. You, D. Wu, H. Liu, Electrochemical studies of molybdate and thiomolybdates. *Polyhedron* ***5***, 535-537 (1986).

30. S. I. Zabinsky, J. J. Rehr, A. Ankudinov, R. C. Albers, M. J. Eller, Multiple-scattering calculations of X-ray-absorption spectra. *Phys. Rev. B* ***52***, 2995-3009 (1995).

31. S. Ghasemi, S. R. Hosseini, S. Nabipour, P. Asen, Palladium nanoparticles supported on graphene as an efficient electrocatalyst for hydrogen evolution reaction. *Int. J. Hydrog. Energy* ***40***, 16184-16191 (2015).

32. L. D. McPherson, M. Drees, S. I. Khan, T. Strassner, M. M. Abu-Omar, Multielectron atom transfer reactions of perchlorate and other substrates catalyzed by rhenium oxazoline and thiazoline complexes: reaction kinetics, mechanisms, and density functional theory calculations. *Inorg. Chem.* ***43***, 4036-4050 (2004).

11

33. S. Ainsworth, Michaelis-Menten kinetics in *Steady-State Enzyme Kinetics*. (Macmillan Education UK, London, 1977), pp. 43-73.

34. D. Shuai, J. K. Choe, J. R. Shapley, C. J. Werth, Enhanced activity and selectivity of carbon nanofiber supported Pd catalysts for nitrite reduction. *Environ. Sci. Technol.* **46**, 2847-2855 (2012).

35. P. B. Weisz, C. D. Prater, Interpretation of measurements in experimental catalysis. *Adv. Catal.* **6**, 143-195 (1954).

36. C. N. Satterfield, *Mass Transfer in Heterogeneous Catalysis* (MIT Press, Cambridge, MA, 1970).

37. M. G. Davie, M. Reinhard, J. R. Shapley, Metal-catalyzed reduction of N-nitrosodimethylamine with hydrogen in water. *Environ. Sci. Technol.* **40**, 7329-7335 (2006).

38. S. R. Heil, M. Holz, T. M. Kastner, H. Weingärtner, Self-diffusion of the perchlorate ion in aqueous electrolyte solutions measured by [35]Cl NMR spin–echo experiments. *J. Chem. Soc. Faraday Trans.* **91**, 1877-1880 (1995).

39. P. Sänger, W.-D. Deckwer, Liquid—solid mass transfer in aerated suspensions. *Chem. Eng. J.* **22**, 179-186 (1981).

40. Y. Sano, N. Yamaguchi, T. Adachi, Mass transfer coefficients for suspended particles in agitated vessels and bubble columns. *J. Chem. Eng. Japan* **7**, 255-261 (1974).

41. R. L. Bates, P. L. Fondy, R. R. Corpstein, Examination of some geometric parameters of impeller power. *Ind. Eng. Chem. Process. Des. Dev.* **2**, 310-314 (1963).

42. B. Liu, H. Yao, W. Song, L. Jin, I. M. Mosa, J. F. Rusling, S. L. Suib, J. He, Ligand-free noble metal nanocluster catalysts on carbon supports via "soft" nitriding. *J. Am. Chem. Soc.* **138**, 4718-4721 (2016).

43. K. D. Hurley, J. R. Shapley, Efficient heterogeneous catalytic reduction of perchlorate in water. *Environ. Sci. Technol.* **41**, 2044-2049 (2007).

44. J. Liu, M. Han, D. Wu, X. Chen, J. K. Choe, C. J. Werth, T. J. Strathmann, A new bioinspired perchlorate reduction catalyst with significantly enhanced stability via rational tuning of rhenium coordination chemistry and heterogeneous reaction pathway. *Environ. Sci. Technol.* **50**, 5874-5881 (2016).

45. J. K. Choe, J. R. Shapley, T. J. Strathmann, C. J. Werth, Influence of rhenium speciation on the stability and activity of Re/Pd bimetal catalysts used for perchlorate reduction. *Environ. Sci. Technol.* **44**, 4716-4721 (2010).
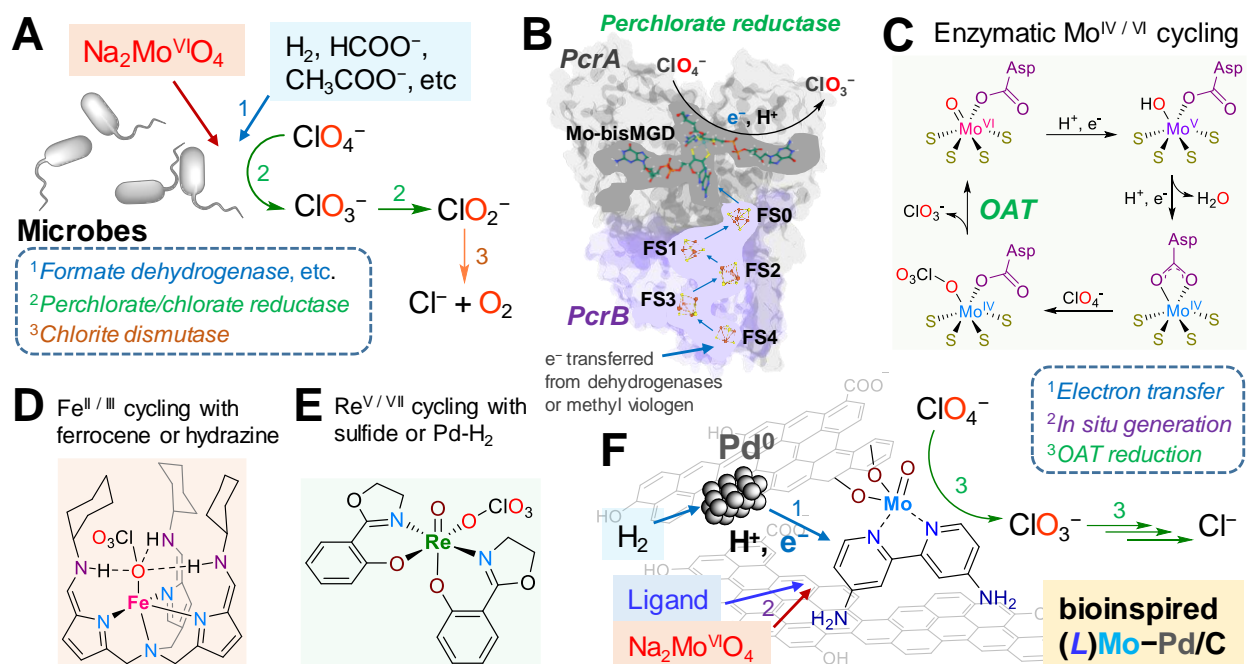
Fig. 1. Comparison of microbial and abiotic systems for perchlorate reduction. (**A**) Microbial process for ClO_4^- reduction; (**B**) electron transfer and metal centers in perchlorate reductase (Pcr); (**C**) proposed redox cycling of the Mo co-factor in reference (*10*); (**D**) a reported bioinspired iron complex for ClO_4^- reduction; (**E**) a reported rhenium complex for ClO_4^- reduction; (**F**) the general working mechanism of the new (*L*)MoO_x−Pd/C catalyst in this study.
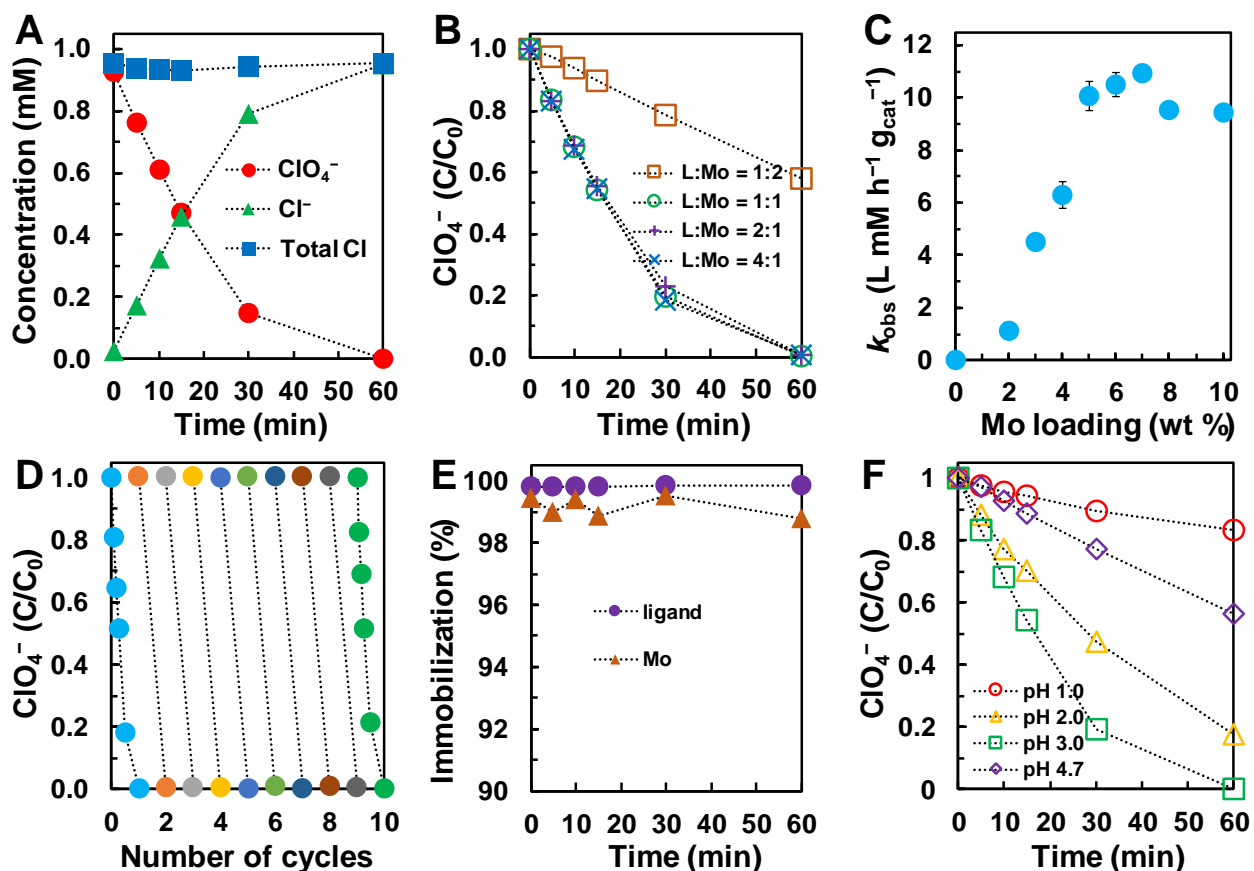
Fig. 2. Kinetics data. **(A)** Chlorine balance during the reduction of ClO_4^-; **(B)** the effect of the different molar ratios of $(NH_2)_2bpy$:Mo; **(C)** the effect of Mo content in the catalyst (y-axis: apparent 0th-order rate constant divided by the catalyst loading); **(D)** performance for ten spikes of 1 mM ClO_4^-; **(E)** the ratio of immobilized ligand and Mo during the reduction of ClO_4^-; **(F)** the effect of solution pH. Default reaction conditions: 0.2 g L^{-1} catalyst (5 wt% Mo in 5 wt% Pd/C, molar ratio of $(NH_2)_2bpy$:Mo=1:1), 1 mM ClO_4^-, pH 3.0, 1 atm H_2, 20 °C.
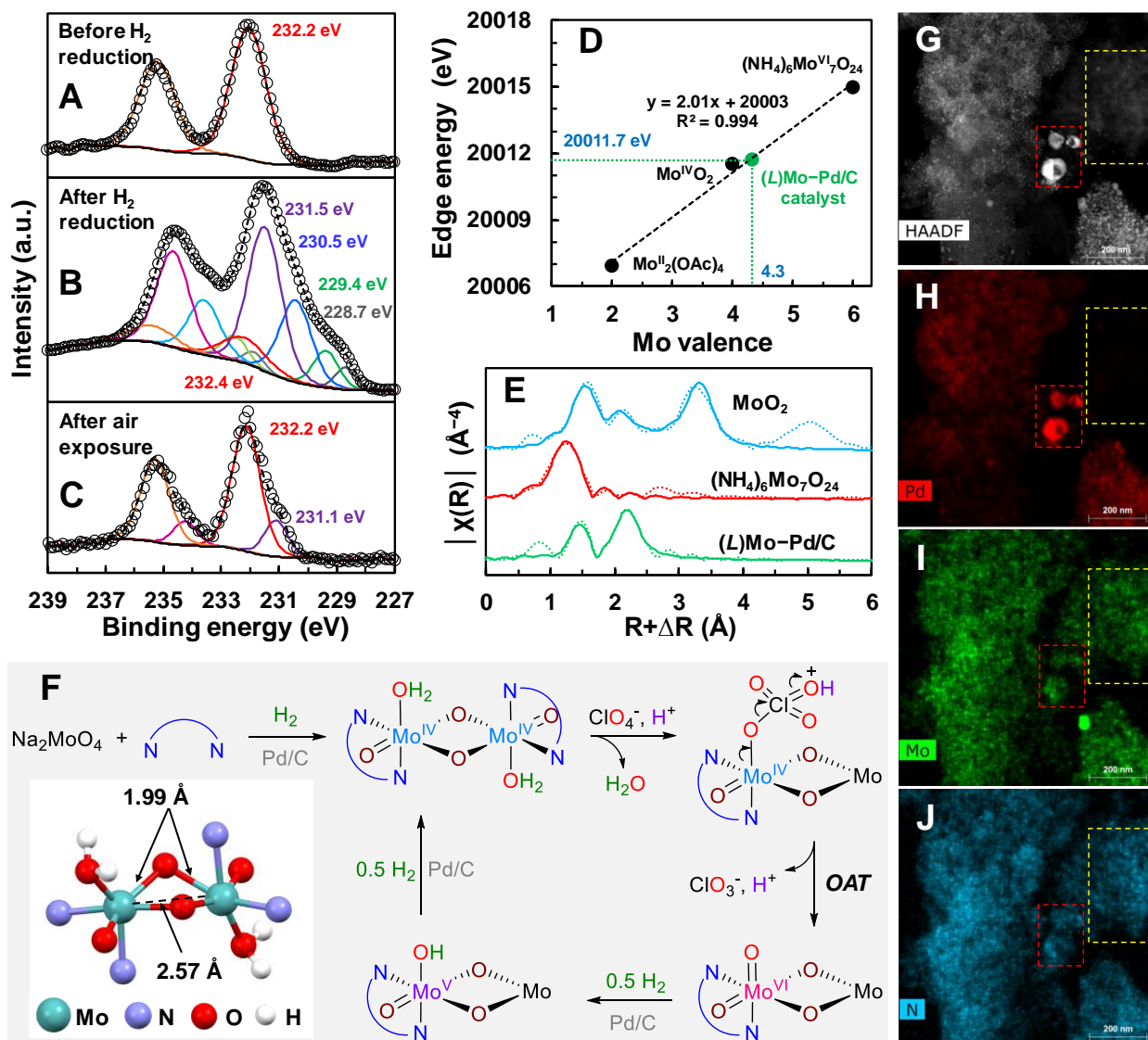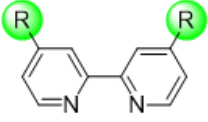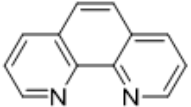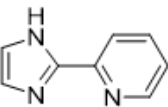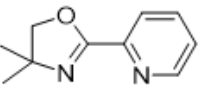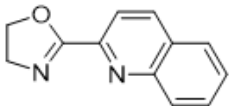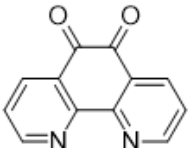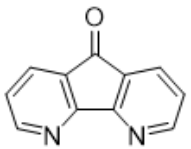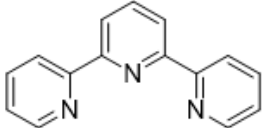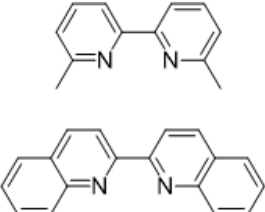
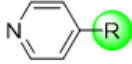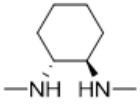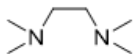**Fig. 3.** Characterization data and proposed reaction mechanisms. **(A−C)** Mo 3d XPS spectra (empty dots) and fits (solid lines) of the $[(NH_2)_2bpy]MoO_x$−Pd/C catalyst; **(D)** the correlation between Mo K-edge XANES energies and valences for the catalyst and Mo references; **(E)** the EXAFS Fourier transforms (dotted lines) and their fits (solid lines); **(F)** a proposed structure of the reduced $[(NH_2)_2bpy]MoO_x$ species and one representative redox transformation for the catalytic reduction of ClO_4^-. **(G−J)** HAADF-STEM imaging of the $[(NH_2)_2bpy]MoO_x$−Pd/C catalyst and EDX mapping of Pd, Mo, and N. The two dotted areas show the heterogeneity of $[(NH_2)_2bpy]MoO_x$ species immobilized on both carbon support and Pd particles.

16

Table 1. Perchlorate Reduction Activity of Mo−Pd/C Catalysts Enabled by Various Nitrogen Ligands.[a]

entry	ligand	TOF$_0$ (h^{-1})[b]	entry	ligand	TOF$_0$ (h^{-1})[b]
	4,4'-R-substituted 2,2'-bipyridine		17	1,10-phenanthroline	3.1
1	R = H	14.3			
2	R = Me	12.4	18	imidazole-pyridine	4.6
3	R = OH	11.7			
4	R = OMe	20.8	19	dimethyl-oxazoline-pyridine	2.8
5	R = NMe$_2$	53.9			
6	R = NH$_2$	106	20	oxazoline-quinoline	0.31
7	R = Cl	0.63			
8	6,6'-dimethyl-2,2'-bipyridine	0.78	21	1,10-phenanthroline-5,6-dione	11.2
9	2,2'-biquinoline	0.13			
	4-R-substituted pyridine		22	indeno-diazafluorenone	0.40
10	R = H	0.16			
11	R = OH	0.16			
12	R = NH$_2$	0.090			
13	R = NMe$_2$	0.79			
14	cyclohexane-1,2-diamine	0.43			
15	ethane-1,2-diamine	0.18			
16	N,N,N',N'-tetramethylethylenediamine	0.22	23	2,2':6',2''-terpyridine	0.85

[a]Reaction conditions: 1 mM ClO$_4^-$ in water, 0.5 g L^{-1} catalyst (5 wt% Mo and 5 wt% Pd on carbon), molar ratio of Ligand:Mo = 1 (bidentate) or 2 (monodentate), pH 3.0, 1 atm H$_2$, 20°C. Entries 5 and 6 used 0.2 g L^{-1} catalyst.

[b]Calculated using the degradation of the first 5% of 1 mM ClO$_4^-$ and four OAT cycles to reduce each ClO$_4^-$ into Cl$^-$.